

## Supplemental Methods and Materials

### Cells and animal model

The embryonal RMS cell line (RME) RD (ATCC, Manassas, VA, USA) and the alveolar RMS (RMA) cell line Rh30 (DSMZ, Braunschweig, Germany) were transduced with a plasmid encoding Gaussia luciferase (GLuc) (pCMV-GLuc, NEB, Frankfurt am Main, Germany). Stable clones expressing GLuc were isolated and maintained in Dulbeccos Modified Eagles Medium (DMEM) supplemented with 10% fetal calf serum (FCS) and the aminoglycoside antibiotic G418 for selection of stable transfected cells. All media and supplements were from Biochrom AG (Berlin, Germany). These cells were transduced with mCherry Lentifect lentiviral particle (GeneCopoeia, Rockville, USA), and red fluorescent cells were selected with 0.3 µg/ml puromycin. Homogenous expression of both transgenes was confirmed by fluorescence microscopy and flow cytometry<sup>1</sup>. Therefore cultured cells were treated with 1 µM Coelenterazine (P.J.K., Kleinblittersdorf, Germany). Green (520 nm) and red (640 nm) fluorescence microscopy was carried out on a Zeiss Axio Scope epifluorescence microscope equipped with MRC5 camera and AxioVision 4.8.1 software (Carl Zeiss, Oberkochen, Germany). Colocalization of GLuc and mCherry was observed by overlapping acquired images. Cells were trypsinated and resuspended in RPMI 1640 medium. To generate a new model of disseminated RMS we established cell lines representing the alveolar (Rh30 cells) and embryonal (RD cells) RMS type with stable expression of the secreted form of the reporter protein GLuc and the intracellular fluorescent protein mCherry. Selection of transduced cells with G418 and puromycin led to a polyclonal cell line with homogenous expression of the reporter genes with comparable growth properties as the parental cell line (data not shown).

10<sup>6</sup> RME or RMA transduced tumor cells in 200 µl were injected i.p. into eight week old NOD/LtSz-scid IL2R $\gamma$ null-mice (NSG, Jackson Laboratories, Bar Harbor, USA). Ten mice were additionally treated 21 days after tumor inoculation (Rh30) with 0.75 µg vincristine/g body weight at two consecutive days. The experimental design is given in the table 1. The animals were kept under pathogen free conditions, fed with an autoclaved standard diet and given free access to autoclaved water. All studies were conducted according to the Guide for the Care and Use of Laboratory Animals (NIH publication 86-23, revised 1985) and with the approval by the responsible animal welfare authority, the German Ethical Committee (Regional Council, approval ID: K 02/10). Serum samples were obtained 14 d and 21 days

after cell inoculation by drawing retro bulbar blood. GLuc activity as relative light units per second (RLU/s) was measured in the serum as described before<sup>2</sup>. Optical imaging and sequential PET/MRI were performed three and four weeks post injection as described below.

### **Optical imaging**

For *in vivo* optical imaging (OI) measurements the fur of the mice was removed with Veet® depilatory cream (Veet, Mannheim, Germany) under inhalative anesthesia using 1.5% isoflurane (Vetland, Louisville, USA) evaporated in 100% medical O<sub>2</sub> at a flow of 0.8 L/min. Fluorescence and bioluminescence signals were detected with the macroscopic imaging system Aequoria™, including the dual mode cooled CCD-Kamera OrcaII-BT1024 and the Hokawo 2.1 software (Hamamatsu Photonics, Herrsching, Germany). Fluorescence-scans for mCherry-detection were acquired using an excitation at 560±40 nm and emission at 630±60 nm with closed aperture, 100% excitation light intensity and 20 s exposure time. At the end of the *in vivo* observation period, animals were sacrificed and optical imaging was repeated using the same settings for fluorescence acquisitions after abdominal exploration and organ resection. Isolated tumors and intraperitoneal tissues were exposed for optical imaging on black paper sheets. *In vivo* and *ex vivo* fluorescence as well as *in vivo* bioluminescence intensity of tumors and organs were quantified with AlphaDigiDoc software (Cell Biosciences, Inc., Santa Clara, USA).

### **PET-Tracer Production**

The radioactive isotopes for the PET-tracers <sup>18</sup>F-FDG, <sup>18</sup>F-FLT, and <sup>11</sup>C-choline, for the detection of intraperitoneal RMS tumors by sequential PET/MRI, were produced with a 16 MeV PETtrace Cyclotron (General Electric Medical Systems, GEMS, Uppsala, Sweden) at the Department of Preclinical Imaging and Radiopharmacy, Tübingen, Germany. A detailed description of the synthesis of each tracer was provided before<sup>3,4</sup>.

Briefly, <sup>18</sup>F-fluoride was produced based on the <sup>18</sup>O(p,n)<sup>18</sup>F nuclear reaction and served for the subsequent radiosynthesis of <sup>18</sup>F-FDG and <sup>18</sup>F-FLT. <sup>18</sup>F-FLT was synthesized using a Tracer LAB FX FN PET tracer Synthesizer (GE Healthcare, Muenster, Germany) with 5'-benzoyl-2,3'-anhydrothymidine as precursor. Mannose triflate (ABX, Radeberg, Germany) was the precursor for the synthesis of <sup>18</sup>F-FDG in a TRACERlab MX synthesizer (GE Healthcare, Breda, Belgium). <sup>11</sup>C-choline was produced based on N,N-dimethylethanolamine (DMAE; Sigma-Aldrich, Munich, Germany) and <sup>11</sup>C-methyl iodide (PETtrace MeI MICROlab, GE Healthcare, Muenster, Germany) in a homemade, automated synthesizer.

## Sequential PET/MRI

For PET-tracer evaluation in the preclinical RMS models, sequential PET/MRI was performed with the tracers  $^{18}\text{F}$ -FDG and  $^{18}\text{F}$ -FLT 3-4 weeks after RMS tumor inoculation.  $^{18}\text{F}$ -FDG-PET/MRI-scans were performed in the morning and  $^{18}\text{F}$ -FLT-PET/MRI scans in the afternoon of the same experimental day. However,  $^{11}\text{C}$ -choline-PET-scans were performed due to logistical issues two days later without MRI in the same animals.

For the evaluation of the effects of cytotoxic agents by PET/MRI, vincristine was administered on two consecutive days three weeks after tumor inoculation as described above. For therapy monitoring, baseline PET/MRI-scans with  $^{18}\text{F}$ -FDG and  $^{18}\text{F}$ -FLT were performed before vincristine treatment.  $^{18}\text{F}$ -FLT- and  $^{18}\text{F}$ -FDG-PET/MRI-scans were repeated two and four weeks after treatment.

All tracers were injected *i.v.* via the lateral tail vein under 1.5% isoflurane anesthesia. We injected 12 MBq  $^{18}\text{F}$ -FDG or  $^{18}\text{F}$ -FLT per mouse in a volume of 25 – 100  $\mu\text{L}$  0.9% NaCl. Static 10 minutes PET-scans with  $^{18}\text{F}$ -FLT were performed after an uptake time of 1.5 h, whereas the uptake time for  $^{18}\text{F}$ -FDG was 1 h. During the  $^{18}\text{F}$ -FLT uptake period animals were awake and during  $^{18}\text{F}$ -FDG uptake the animals were anesthetized and heated on a heating mat. Additionally, the animals were fasted prior to the injection of  $^{18}\text{F}$ -FDG for 8-10 hours. Static  $^{11}\text{C}$ -cholin PET images were acquired for 10 min after injection of 4 MBq tracer and a 10 min uptake period. Animals were kept under anesthesia and were warmed during uptake and scan time.

*In vivo* PET scans were acquired with a small-animal Inveon microPET scanner (Siemens Medical Solutions, Knoxville, USA). The axial field of view (FOV) of the scanner was 12.7 cm, the transaxial FOV 10 cm<sup>5</sup>. The PET-scans were acquired in listmode format and reconstructed using a 2D iterative Ordered Subset Expectation Maximization (2DOSEM) algorithm, resulting in a spatial resolution of the reconstructed PET images of approximately 1.4 mm. Glass capillaries were filled with small amounts of the respective tracer and fixed on the mouse bed. These markers enabled the co-registration of PET- and MRI-scans during data-analysis.

After the PET-scans, animals were transferred fixated on the mouse bed to a dedicated 7-T small animal MR scanner (ClinScan, Bruker Biospin MRI GmbH, Ettlingen, Germany) equipped with a quadrature mouse whole-body coil (diameter 35 mm). For the detection of the tumors, a T2-weighted 3D turbo-spin echo sequence was applied (TR: 3000 ms, TE: 205

ms, voxel size: 0.22x0.22x0.22 mm<sup>3</sup>). To minimize motion artifacts caused by breathing, scans were triggered on the respiration of the animals using a monitoring unit (SAInstruments, Stony Brook, USA).

Reconstructed PET-images were corrected for radioactive decay and normalized to the injected activity. According to our standard PET protocol for mice, attenuation correction was not applied. Using the analysis software Inveon Research Workplace (IRW, Siemens), the PET-images were co-registered with the corresponding MR-scans. Volumes of interests (VOI) were drawn in the PET images on the intraperitoneal RMS tumors based on the anatomical information of the MRI-scan. For data analysis the %-injected dose per cm<sup>3</sup> (%ID/cc) was calculated.

### **Biodistribution**

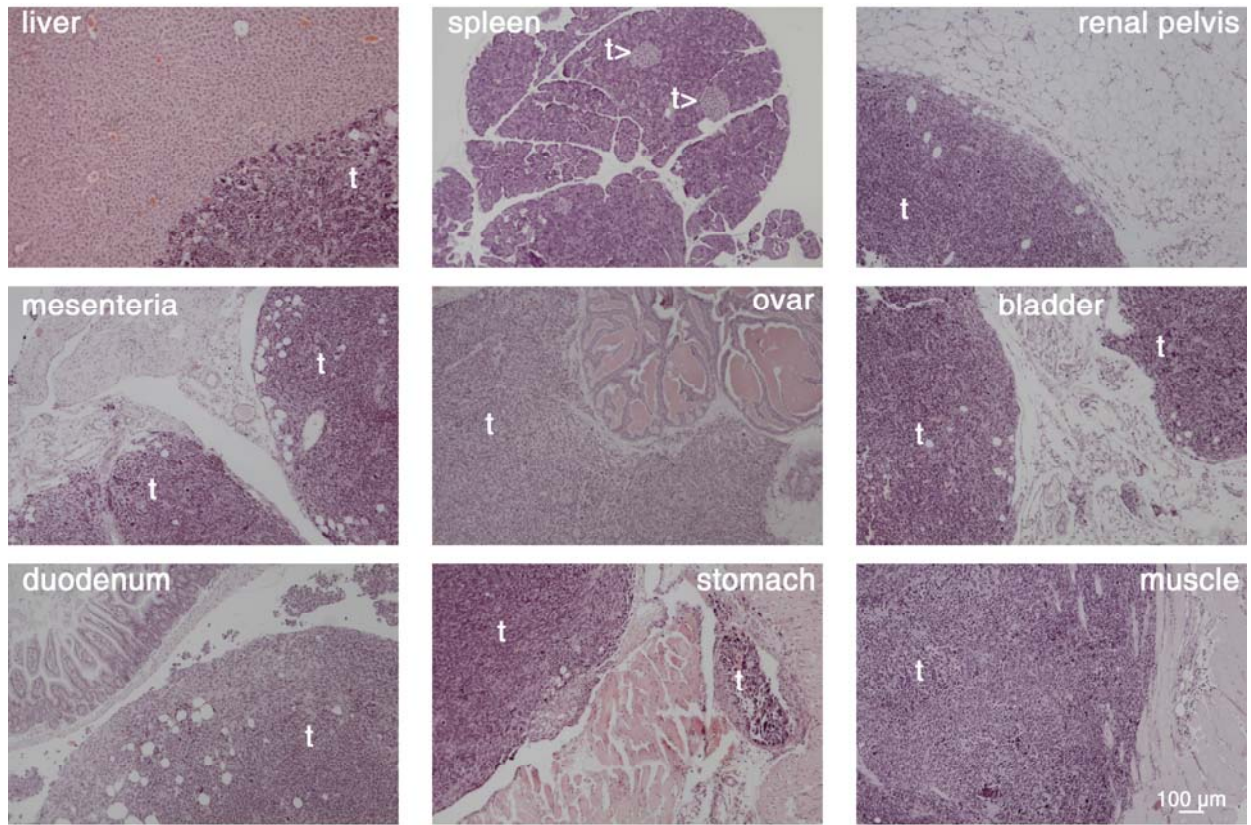
In a separate experiment, we wanted to characterize the uptake patterns of <sup>18</sup>F-FDG and <sup>18</sup>F-FLT in Rh30-tumors ex vivo by biodistribution to confirm the in vivo PET/MRI-results. Therefore, an additional of 8 Rh30-bearing experimental mice were injected with <sup>18</sup>F-FDG (n=4) or <sup>18</sup>F-FLT (n=4) 3 weeks after the i.p. tumor inoculation and tumors were explanted and weighed after the uptake period of the respective PET-tracer. Animals were sacrificed and RMS tumors as well as muscle tissue were isolated. Ex vivo fluorescence OI scans of the dissected Rh30-tumors were performed before the activity in the tumors was determined using a  $\gamma$ -counter (Perkin Elmer, Waltham, USA), with an energy window between 350 and 650 keV. We calculated the injected dose per gram (%ID/g) by normalizing the acquired counts to the injected dose of the respective tracer and the weight of the tumors.

### **Histological and immunohistological analysis**

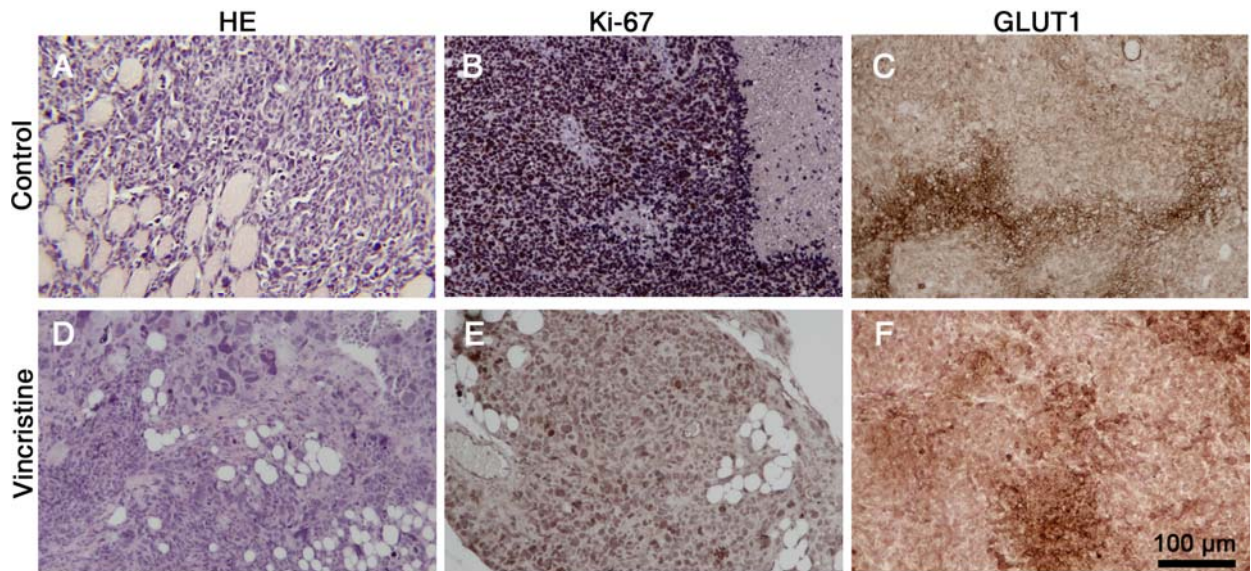
Tumor tissues were fixed in 3.7% formalin and processed for further histological analysis as described before<sup>6</sup>. Sections of 3  $\mu$ m were stained with hematoxylin/eosin. Immunohistochemistry of paraffin embedded sections was performed using the ABC method as described previously with the following antibodies: Ki-67 (DAKO, Hamburg, Germany) and Glucose Transporter 1 (Thermo Fischer, Schwerte, Germany)<sup>7</sup>. Microscopy was carried out using a Zeiss Axio Scope microscope (Carl Zeiss, Oberkochen, Germany). Images were taken with the Canon 550D camera and processed using AxioVision 4.8.1 software.

### **Statistical analysis**

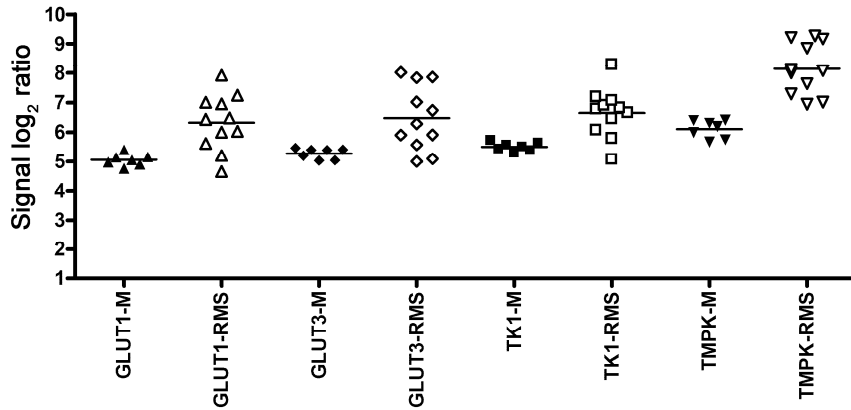
Statistical analysis was performed by one way ANOVA on ranks test and student's two-tailed t-test. All numeric data are expressed as mean  $\pm$  SD. Significance was assumed for all  $p < 0.05$ . Linear regression analysis was done using GraphPad Prism (GraphPad Software, San Diego, USA).



Supplemental Figure 1. Histological evaluation of tumors isolated from liver, spleen, renal pelvis, mesenteria, ovar, bladder, duodenum, stomach and muscle showed homogenous cell distribution with few necrotic areas (HE staining).

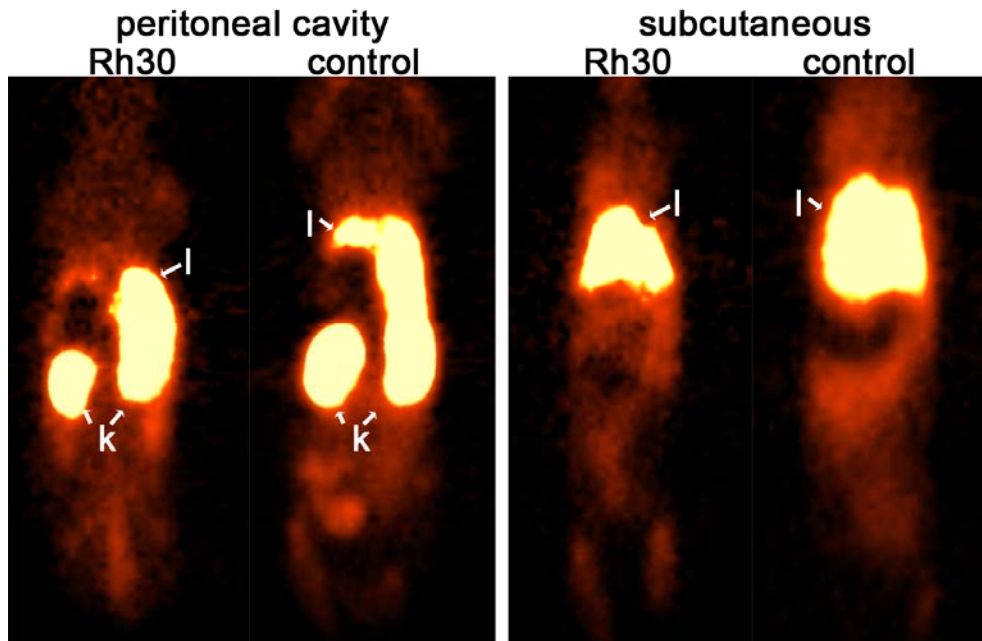


Supplemental Figure 2. Histological evaluation of Rh30 tumors after treatment with vincristine. Tumors from control mice (A-C) and from vincristine treated mice (D-F) were analysed by HE staining (A/D), Ki-67 (B/E) and GLUT1 (D/F) immunohistochemistry. Histological evaluation of tumors treated with vincristine showed homogenous cell distribution of anaplastic cells (D). Ki-67 positive cells were stained brown. GLUT1 was detected as brown staining on cell surface in isolated regions within the tumor nodules.

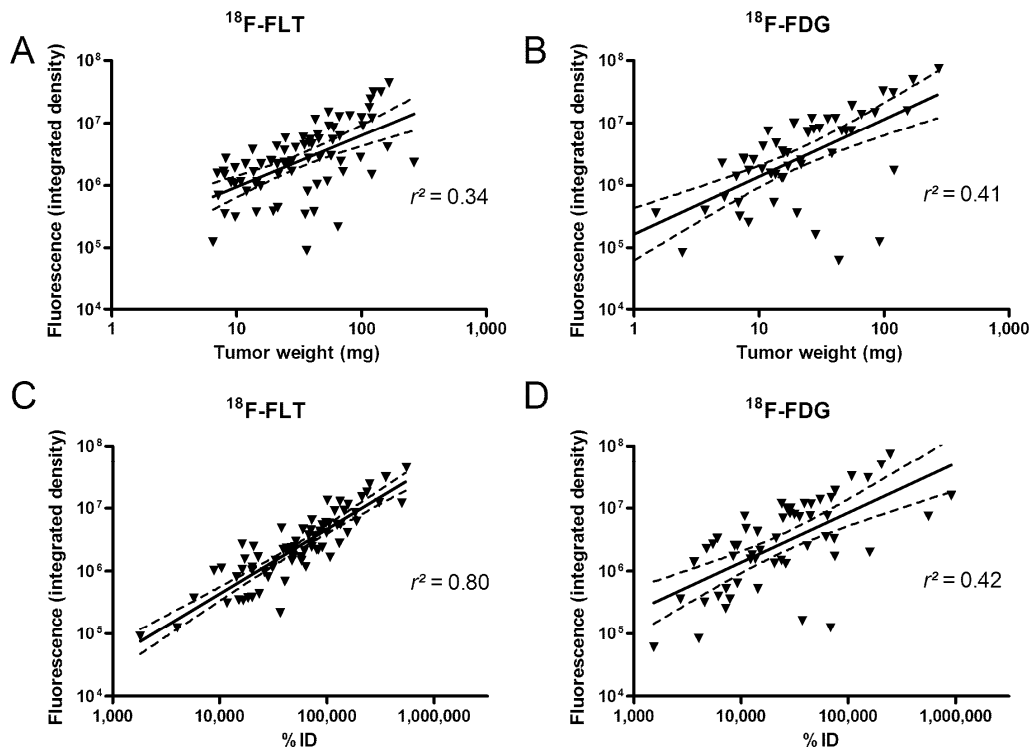


Supplemental Figure 3. Expression of glucose transporters and kinases in Rh30-RMS cells and muscle tissue. Gene expression analysis revealed a differential expression of genes coding for glucose transporters (GLUT1 and GLUT3) and enzymes involved in retention of thymidine in cells (thymidine kinase 1 (TK1) and thymidine monophosphate kinase (TMPK)) are overexpressed in RMS. Relative signal intensity of the probe sets from Affymetrix high-density oligonucleotide microarrays (GeneChip® Human Genome U133 Plus 2.0 Array) for each tissue sample are shown. Own published database<sup>8</sup>





Supplemental Figure 4. Detection of Rh30 tumors by  $^{11}\text{C}$ -choline-PET. No uptake of  $^{11}\text{C}$ -choline was observed in peritoneal and subcutaneous Rh30 tumors. Presented are the identical experimental and control animals as shown in figure 3. High uptake in liver (l) and kidneys (k) was observed in control mice without tumors (control) in the PET images.



Supplemental Figure 5. Comparison of the  $^{18}\text{F}$ -FLT and  $^{18}\text{F}$ -FDG tracers for the detection of Rh30 tumors. Tumors were detected in 9 mice using PET/MRI. Rh30 tumors were evaluated at necropsy to analyze the uptake of  $^{18}\text{F}$ -FDG (44 tumors) and  $^{18}\text{F}$ -FLT (36 tumors) by fluorescence-OI (A,B). A linear correlation of fluorescence intensity with the tumor weight and with the incorporated activity (%ID) was observed (C,D).

1. Armeanu-Ebinger S, Wenz J, Seitz G, et al. Characterisation of the cell line HC-AFW1 derived from a pediatric hepatocellular carcinoma. *Plos One*. 2012;7.
2. Lieber J, Eicher C, Wenz J, et al. The BH3 mimetic ABT-737 increases treatment efficiency of paclitaxel against hepatoblastoma. *BMC Cancer*. 2011;11.
3. Kukuk D, Reischl G, Raguin O, et al. Assessment of PET tracer uptake in hormone-independent and hormone-dependent xenograft prostate cancer mouse models. *J Nucl Med*. 2011;52:1654-1663.
4. Reischl G, Bieg C, Schmiedl O, Solbach C, Machulla HJ. Highly efficient automated synthesis of (11)C-choline for multi dose utilization. *Appl Radiat Isot*. 2004;60:835-838.
5. Mannheim JG, Judenhofer MS, Schmid A, et al. Quantification accuracy and partial volume effect in dependence of the attenuation correction of a state-of-the-art small animal PET scanner. *Phys Med Biol*. 2012;57:3981-3993.
6. Seitz G, Armeanu-Ebinger S, Warmann S, Fuchs J. Animal models of extracranial pediatric solid tumors. *Oncol Lett*. 2012;4:859-864.
7. Seitz G, Pfeiffer M, Fuchs J, et al. Establishment of a rhabdomyosarcoma xenograft model in human-adapted mice. *Oncol Rep*. 2010;24:1067-1072.
8. Herrmann D, Seitz G, Warmann SW, Bonin M, Fuchs JR, Armeanu-Ebinger S. Cetuximab promotes immunotoxicity against rhabdomyosarcoma in vitro. *J Immunother*. 2010;33:279-286.